/
Article / Book Information

Title	Room-temperature ultraviolet laser emission from self-assembled ZnO microcrystallite thin films
Authors	Z. K. Tang,G. K. L. Wong,P. Yu,M. Kawasaki,A. Ohtomo,H. Koinuma,Y. Segawa
Citation	Applied Physics Letters, Vol. 72, No. 25,
Pub. date	1998, 6
URL	http://scitation.aip.org/content/aip/journal/apl
Copyright	Copyright (c) 1998 American Institute of Physics

Room-temperature ultraviolet laser emission from self-assembled ZnO microcrystallite thin films

Z. K. Tang,[a] G. K. L. Wong, and P. Yu
*Physics Department, Hong Kong University of Science and Technology, Clear Water Bay,
Kowloon, Hong Kong*

M. Kawasaki, A. Ohtomo, and H. Koinuma
*Materials and Structures Laboratory, Tokyo Institute of Technology, Nagatsuda, Midori-ku,
Yokohama 227, Japan*

Y. Segawa
*Photodynamics Research Center, The Institute of Physical and Chemical Research (RIKEN),
19-1399 Nagamachi Koeji, Aoba-ku, Sendai 980, Japan*

Room-temperature ultraviolet (UV) laser emission of ZnO microcrystallite thin films is reported. The hexagonal ZnO microcrystallites are grown by laser molecular beam epitaxy. They are self-assembled and parallelly arrayed on sapphire substrates. The facets of the hexagons form natural Fabry–Pérot lasing cavities. The optical gain for the room-temperature UV stimulated emission is of an excitonic nature and has a peak value an order of magnitude larger than that of bulk ZnO crystal. The observation of room-temperature UV lasing from the ordered, nano-sized ZnO crystals represents an important step towards the development of nanometer photoelectronics. © *1998 American Institute of Physics.* [S0003-6951(98)03325-7]

In recent years, wide-gap semiconductor compounds have attracted a great deal of attention because of the intense commercial interest in developing practical short-wavelength semiconductor diode lasers (SDLs) for the huge market needs. World-wide research efforts on the development of short-wavelength SDLs were initially focused on ZnSe-based heterostructures, but recently the interest in InGaN materials has grown considerably. These developments have culminated in the demonstration of room-temperature operating green–blue as well as blue SDL structures.[1–3] ZnO is another wide-gap semiconductor, but it has received surprisingly little attention despite its large exciton binding energy of 60 meV, which in principle should allow efficient excitonic lasing mechanisms to operate at room temperature (RT). Ultraviolet (UV) stimulated emission and lasing have been extensively studied in bulk ZnO crystals at cryogenic temperatures,[4–7] but observation of lasing at RT was mentioned only briefly in the works of Klingshirn[7] and in very recent reports.[8–10]

We report RT UV lasing from ZnO thin films that were grown on sapphire (0001) substrates. As a result of the large lattice mismatch, these films consist of an epitaxially ordered array of hexagonal microcrystallites. The facets of all hexagons are parallel to those of the others, forming natural Fabry–Pérot lasing cavities. Under moderate excitation, the optical gain responsible for the RT UV stimulated emission is of an excitonic nature. For a 55-nm-thick film, an excitonic gain of 320 cm^{-1} is measured at a fluence of $3.0 \ \mu \text{J/cm}^2$, an order of magnitude larger than the gain reported for bulk ZnO crystals measured at much higher fluence.[11]

The growth of ZnO thin films on sapphire substrate and their linear optical spectra were reported many years ago by some research groups.[12] In this work, self-assembled ZnO microcrystallites were grown on sapphire substrates by the laser molecular beam epitaxy technique,[13] at a deposition temperature of 500 °C and an oxygen pressure of 1×10^{-6} Torr. A pure ceramic ZnO target (99.999%) was ablated in an ultrahigh vacuum chamber using a KrF excimer laser. X-ray diffraction measurement revealed that the ZnO microcrystallites have high crystallinity with c-axis orientation. Figure 1 shows the atomic force microscope (AFM) topography of a ZnO thin film with a thickness of 200 nm. The thin film consists of close-packed hexagons. The hexagonal column structure is also confirmed by transmission electron microscope TEM observation.[14] The facets of the hexagons correspond to the {1100} plane and they are strictly
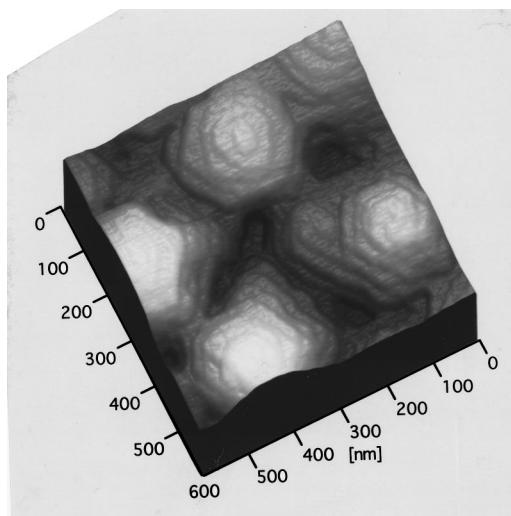

FIG. 1. AFM topograph of a ZnO epitaxial film grown on a sapphire (0001) substrate.
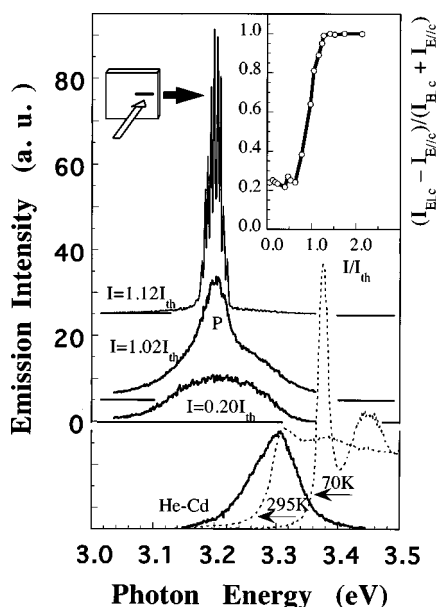
FIG. 2. The lower trace shows the absorption spectrum (dotted curve) and photoluminescence spectrum, measured at 70 K and room temperature, respectively. The upper traces show spontaneous and stimulated emission spectra under pumping intensities of $0.2I_{th}$, $1.02I_{th}$ and $1.12I_{th}$ provided by the frequency-tripled and mode-locked Nd:YAG laser (355 nm, 15 ps). The inset at right side shows the degree of polarization of the UV emissions plotted as a function of the pumping intensity.
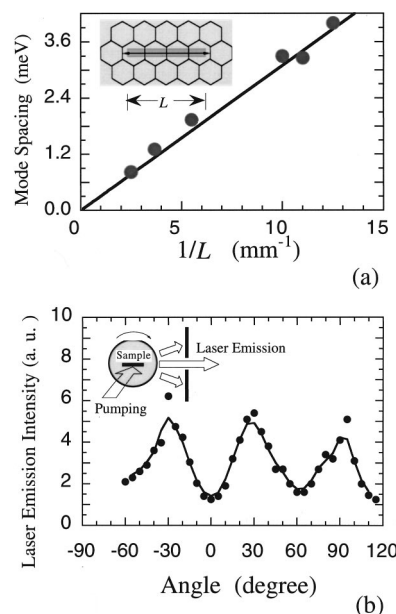

FIG. 3. (a) The mode spacing (solid circles) plotted as a function of the stripe length L of the pumping laser beam. The solid line is calculated for a Fabry–Pérot resonant cavity with length L. A model of natural Fabry–Pérot microcavity formed by the hexagonal microcrystallites is schematically drawn in the inset. (b) The laser emission intensity plotted as a function of rotating angle. The experimental setup is shown in the inset. The maximum and the minimum of the laser emission intensity repeats every 60°.

parallel to the {1120} plane of the sapphire substrate.

The lower trace in Fig. 2 shows the absorption spectrum (dotted curve) measured at 70 and 295 K, respectively, as well as the photoluminescence spectrum (solid curve) measured using the 325 nm line of a continuous wave (cw) He–Cd laser in a backscattering configuration at 295 K for a 55-nm-thick ZnO thin film. The AFM topography (not shown here) reveals that the microcrystallite size of this film is about 50 nm in diameter. At 70 K, a pronounced free $1s$ exciton absorption peak (A) is observed at 3.38 eV. The free-exciton energy shifted to 3.31 eV at room temperature. An intense free-exciton emission (E_{ex}), slightly Stokes-shifted from the absorption peak, is seen at room temperature. The upper traces in Fig. 2 show the emission spectra pumped at below, near, and above a threshold, $I_{th}=40$ kW/cm^2, for stimulated emission, using the frequency-tripled output (355 nm) from a pulsed Nd:YAG laser (15 ps, 10 Hz) in a configuration shown in the inset. At low pumping intensities, a broad emission band is observed at 3.2 eV which is lower than E_{ex} by about 110 meV. The intensity of this emission band increases quadratically when the pumping intensity is below the I_{th}, in contrast to the linear increase in the free-exciton emission intensity. When the ZnO film is pumped at an intensity just above the threshold, $I=1.02I_{th}$, a narrow emission band P emerges directly from the broad spontaneous spectrum. The P band grows superlinearly with pumping intensity. At a higher pumping intensity ($I=1.12I_{th}$), many sharp lines equally spaced in energy appear in the emission spectrum. The inset on the right side of Fig. 2 shows the degree of polarization, $(I_{E\perp c}-I_{E\parallel c})/(I_{E\perp c}+I_{E\parallel c})$, for the emission band as a function of the pumping intensity, here $I_{E\perp c}$ and $I_{E\parallel c}$ are the integrated intensities of the $E\perp c$ and $E\parallel c$ polarized emissions, respectively. Below I_{th}, the $E\perp c$ and $E\parallel c$ polarized emission bands have nearly equal intensi-

ties. The degree of polarization increases quickly near the threshold, and tends to unity when the pumping intensity is higher than I_{th}, indicating that the emission is highly $E\perp c$ polarized at above threshold pumping. The above observations indicates unequivocally that RT UV lasing occurred in these ZnO microcrystallites.

The regularly spaced sharp lines in the lasing spectrum look like cavity modes. However, since we did not intentionally form a lasing cavity, it was not clear where the required feedback came from. The line spacing is measured under different pumping stripe lengths, and is plotted in Fig. 3(a) as a function of the reciprocal stripe length L. The solid line shown in Fig. 3(a) is calculated for a Fabry–Pérot resonant cavity with length L, using equation $\Delta E=(\pi ch/L)(n+Edn/dE)^{-1}$, where $E(dn/dE)$ is the variation of the refractive index n with photon energy E. The data of the refractive index $n(E)$ is obtained from Ref. 15. The good agreement between the calculated values and the measured spacing between the cavity modes strongly indicates that the sharp lines are due to the longitudinal modes of an optical cavity having a cavity length equal to the entire excitation stripe. We propose that a laser cavity is formed by the {1100} facets of the parallelly arrayed hexagonal ZnO microcrystallites, as schematically shown in the inset of Fig. 3(a). Many such hexagons are expected to be covered by the pumping stripe. Within the pumping region, the high density of excitons created in the microcrystallites by the photoexcitation leads to a decrease of the refractive index because of the exciton phase space filling effect. Hence, a significant reflectivity can occur at the two ends of the pumping stripe, while the reflections at the boundaries between grains inside or outside the pumping region should be negligible because of the same refractive index between those grains. To confirm

our microcavity model, we measured the laser emission intensity by rotating the sample using the experimental configuration shown by the inset of Fig. 3(b). The intensity is plotted in Fig. 3(b) as a function of the angle of rotation. The maximum or the minimum of the lasing intensity repeat every 60°, which indicates that the laser cavity is formed by the parallel facets of the hexagonal ZnO microcrystallites. It is worth pointing out that the angle dependence of the lasing intensity can come also from scattering losses which depend on the orientation of wave vector **K** relative to the hexagons. However, without the hexagonal cavity model, we cannot explain where the equal-spaced lasing modes come from.

The pumping induced reflectivity R at the two facets near the end of the pumping stripe can be approximately estimated from the refractive index $n_{ex} = 2.45$ for the lasing light with energy of 3.2 eV and the refractive index 1.92 for the light far away from the exciton resonance.[15] Under high pumping conditions, the refractive index near the excitonic resonant energy can be decreased due to the exciton bleaching effect. Hence, the largest change in the refractive index due to the high intensity pumping is expected to be $\Delta n = -0.53$, which can give rise to a reflectivity of about 1.5%. The strong contrast of the observed Fabry–Pérot oscillations (Fig. 2) cannot be explained by such a small reflectivity without the presence of a large optical gain. We measured gain spectra[16] using variable stripe length by carefully taking the pumping saturation effect into account. The measured peak gain reaches a value of $320 \ cm^{-1}$ at a fluence of $3.0 \ \mu J/cm^2$. This peak gain value is nearly one order of magnitude larger than that of bulk ZnO crystals measured at much higher excitation intensity.[11]

Large optical gain and low lasing threshold are two important factors for practical SDL applications. A clear understanding of the microscopic mechanism responsible for optical gain and stimulated emission is important for such optimization. Figure 4 shows the laser emission spectra measured under higher pumping intensities. At a moderate pumping intensity, only the lasing lines grouped by P are seen in the spectrum (the lowest spectrum in Fig. 4). As the pumping intensity is increased, we can observe another lasing group marked by N. The integrated lasing intensity of the P group decreases when the pumping intensity is higher than $1.4 I_{th}$, while the N group starts to appear at the low energy side of the P group. It is noted that there is no remarkable spectral shift of the P lasing group at various pumping intensities. In contrast, the central position of the N lasing group shifts towards the lower energy as the pumping intensity is increased. Obviously, the P group and the N group emission lines are of different origins. The pumping intensity at $1.4 I_{th}$ corresponds to an electron–hole pair density of $10^{18} \ cm^{-3}$, which is near the Mott transition density for bulk ZnO. When the pumping intensity changed from $1.44 I_{th}$ to $2.73 I_{th}$, the N band down-shifted from 3.175 to 3.145 eV by 30 meV, which is in good agreement with the redshift of the electron–hole plasma (EHP) observed in bulk ZnO.[17] Hence, the N group lasing can be reasonably attributed to the EHP radiative recombination. On the other hand, the lack of substantial spectral shift of the P lasing group indicates its optical gain is of excitonic nature. We attribute the RT UV stimulated emission in the ZnO microcrystallites to the radiative recom-
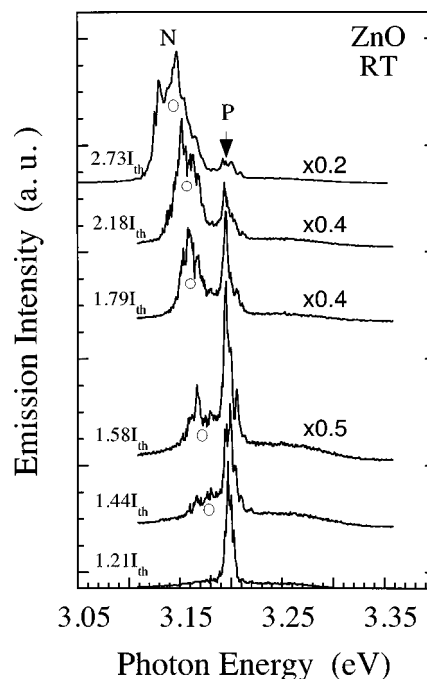

FIG. 4. Lasing spectra of the ZnO microcrystallite film pumped using the frequency-tripled output of a mode-locked Nd:YAG laser at various pumping intensities.

bination process of the exciton–exciton collision as discussed in Ref. 18 in detail.

[1] H. Jeon, J. Ding, A. V. Nurmikko, H. Luo, N. Samarth, J. K. Furdyna, W. A. Bonner, and R. E. Nahory, Appl. Phys. Lett. **57**, 2413 (1990).
[2] M. A. Haase, J. Qui, J. M. De Puydt, and H. Cheng, Appl. Phys. Lett. **59**, 1272 (1991).
[3] S. Nakamura, M. Senoh, S. Nakahana, N. Iwasa, T. Yamada, T. Matsushita, Y. Sugimoto, and H. Kiyoku, Appl. Phys. Lett. **69**, 1477 (1996).
[4] J. M. Hvam, Phys. Rev. B **4**, 4459 (1971); Phys. Status Solidi B **63**, 511 (1974).
[5] H. Huang and S. Kock, Phys. Status Solidi B **82**, 531 (1975).
[6] C. Klingshirn, Adv. Mater. Opt. Electron. **3**, 103 (1994); Solid State Commun. **13**, 297 (1973).
[7] C. Klingshirn, Phys. Status Solidi B **71**, 547 (1975); **89**, 431 (1978).
[8] D. M. Bagall, Y. F. Chen, Z. Zhu, T. Yao, S. Koyama, M. Y. Shen, and T. Goto, Appl. Phys. Lett. **70**, 2230 (1997).
[9] Z. K. Tang, P. Yu, G. K. L. Wong, M. Kawasaki, A. Ohtomo, H. Koinuma, and Y. Segawa, Solid State Commun. **103**, 459 (1997).
[10] Z. K. Tang, P. Yu, G. K. L. Wong, M. Kawasaki, A. Ohtomo, H. Koinuma, and Y. Segawa, Nonlinear Opt. **18**, 355 (1997).
[11] J. M. Hvam, J. Appl. Phys. **49**, 3124 (1978).
[12] See, for example, H. Schneck and R. Helbig, Thin Solid Films **27**, 101 (1975); E. Mollwo *et al.*, Series Solid State Physics (Seitz-Turnbull Series) **8**, 216 (1959).
[13] H. Koinuma and M. Yoshimoto, Appl. Surf. Sci. **75**, 308 (1994).
[14] N. Wang, K. K. Fung, P. Yu, Z. K. Tang, G. K. L. Wong, M. Kawasaki, A. Ohtomo, H. Koinuma, and Y. Segawa, Mater. Res. Soc. Symp. Proc. **482**, (1997).
[15] W. L. Bond, J. Appl. Phys. **36**, 1674 (1965).
[16] P. Yu, Z. K. Tang, G. K. L. Wong, M. Kawasaki, A. Ohtomo, H. Koinuma, and Y. Segawa, The 8th International Conference on II-VI Compounds, Grenable, France, 25–29 August, 1997.
[17] C. Klingshirn, J. Cryst. Growth **117**, 753 (1992).
[18] P. Yu, Z. K. Tang, G. K. L. Wong, M. Kawasaki, and Y. Segawa, Proceeding of the 23rd International Conference on the Physics of Semiconductors, 1996, Vol. 2, p. 1453.